

A NEW DISTANCE PROTECTION SCHEME BASED ON COMBINATION OF IMPEDANCE AND TRAVELLING WAVE MEASUREMENTS

Rasha Mansour¹, Elsayed Hassan Shehab-Eldin², M. Elshahat Masoud³

ABSTRACT

In this technique the relay can detect the fault and can discriminate between internal and external fault without the need for communication links. That combines of both impedance based methods and traveling wave based methods has been developed and presented in this paper. The proposed method first determines whether the fault is backward or forward to the measured relay and then determines if the fault is grounded or ungrounded. Next, the impedance based method is used to identify the fault for ungrounded faulted. Finally the traveling wave method is used to detect the fault for grounded fault by using the ground and Ariel mode. The simulation results indicate a good accuracy and more security of the suggested protection scheme compared with others schemes with different types of faults, fault resistances and fault inception angles using MATLAB/SIMLINK simulation.

Keywords: Travelling wave protection, Discrete Wavelet Transform and Distance protection.

1. INTRODUCTION

A perfect transmission line protection scheme is expected to differentiate the internal faults from external precisely so that only the faulted line will be removed.

Contemporary techniques for power line protection can be broadly classified into two categories, the non-unit and unit protection [1]. For many years, extensive research has been conducted to improve the two techniques. However, each technique has its own limitation. The disadvantage of non unit schemes, such as distance protection, is that it cannot protect the entire line. In this respect, unit schemes such as current differential protection solve this problem, but they require very expensive and sophisticated communication channels between the line ends. Moreover, the reliability of the technique will also depend on the reliability of the communication link and device [2].

Conventional method of distance protection is to use the voltage and current data measured at one or more points along the power networks. Knowing the line impedance per unit length, the fault distance can be approximated from the calculated impedance obtained from the voltage and current data. This impedance method, however, is subject to errors caused by for example high resistance ground faults, teed circuits topologies, and the interconnection to multiple sources [3].

The other technique used is the travelling waves method [4-12]. In all these techniques, the high frequency transients are used instead of the steady state components to determine the location of the fault. Single-ended and double-ended techniques have been used to determine the fault location using travelling waves [13]. For single-ended, the current or voltage signals are measured at one end of the line and fault location relies on the analysis of these signals to detect the reflections that occur between the measuring point and the fault.

Such algorithms have been noted as being too complex and erroneous for operations personnel to accurately locate faults [14] due to the problems with distinguishing between traveling waves reflected from the fault and from the remote end of the line [15]. In some situations, it may also be difficult to identify the true wavefront of the recorded signal as the transient can become lost in the disturbances created by a previous event [16].

In order to improve the power reliability, a variety of protection devices are developed such as fault locator which is proposed in literatures. Accurate fault location reduces time and costs related to the dispatched crews searching to find the fault location [17]. Also, provides customers and consumers feeding with minimal interruption and improves the performance of the power system [18]. Fault location methods that are used to find location of fault in the transmission lines are classified into two general categories [19]:

- 1- Impedance-based methods
- 2- Travelling waves-based methods [20]

The combination between travelling wave algorithm and impedance measurement technique in a single

*1Helwan machinery and equipment Company, Cairo, Egypt,
E-mail: rasha_mansour_82@yahoo.com*

2Department of Electrical Machines & Power Engineering, Helwan University, Cairo, Egypt, E-mail: shehab_eldin01@yahoo.com

3 Department of Electrical Machines & Power Engineering, Helwan University, Cairo, Egypt-mail: dr_masoud@yahoo.com

relay. The travelling wave information is used to achieve fast fault detection speeds for grounded faults while the impedance measurement is used to improve the reliability of the protection scheme for ungrounded faulted phases

The fundamental principle of the proposed fault location algorithm is explained in Section 2. Test systems considered to explain the proposed method is discussed in Section 3 and the conclusion is given in Section 4.

2. FAULT LOCATION METHOD

The algorithm involves three major steps:

- (i) Determination of the fault direction
- (ii) Determination of the fault type
- (iii) Discriminate of the fault position
 - One zone distance protection algorithm
 - Travelling wave algorithm

This has been summarized in the flow chart given in Fig. 1. It is assumed that the measurements are done at all the ends of the line independently (not synchronously) and there is no online communication between the terminals. Therefore, this method can also be termed as a one-end method

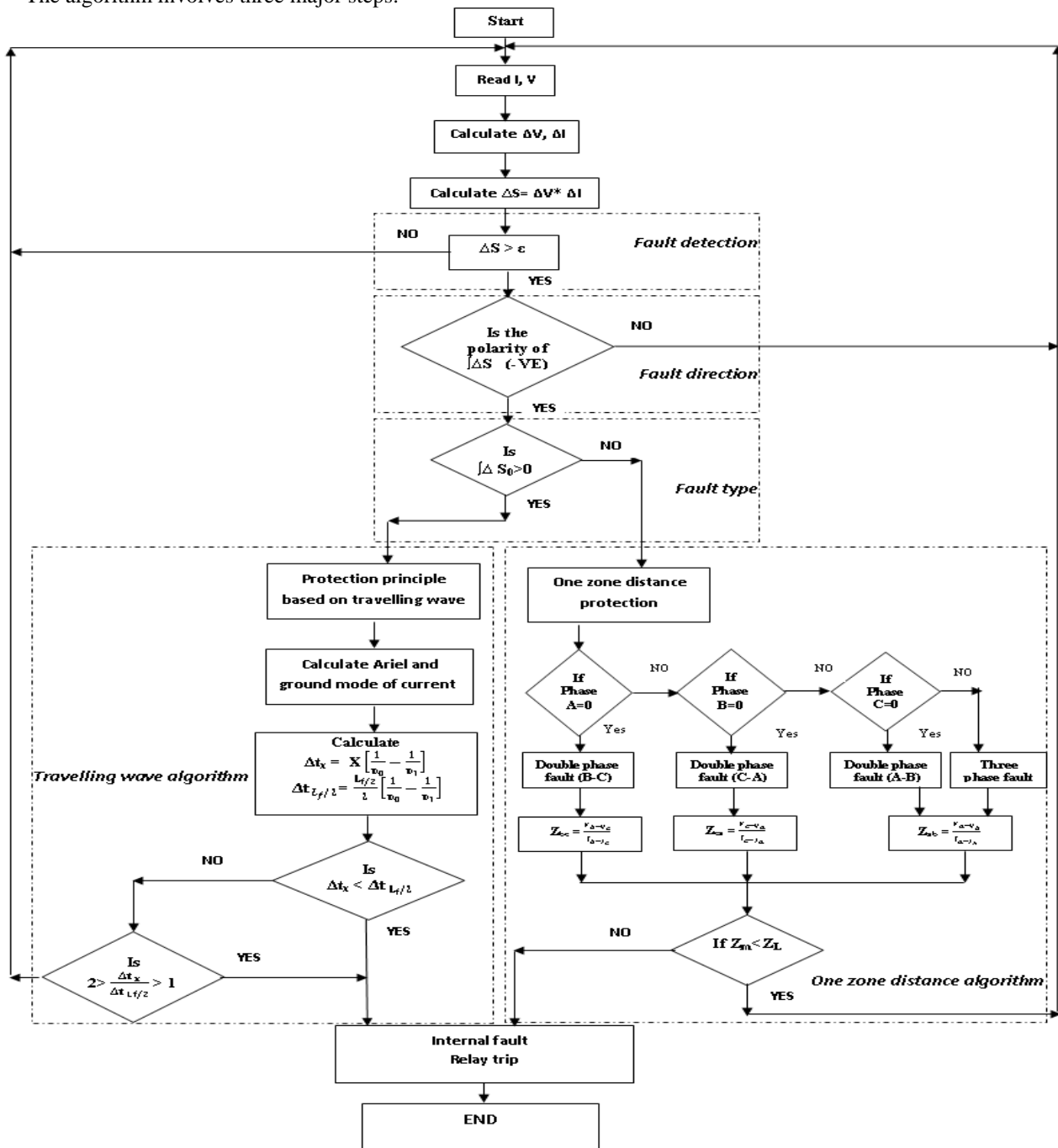


Figure 1 Flow chart of the combination between impedance and travelling wave algorithm

2.1. Determination of the Fault Direction

To determine the fault direction and discriminate if it is forward or backward fault is performed by this equation

$$\Delta S = \int \Delta V \times \Delta I \quad (1)$$

Where $\Delta V = V \text{ post} - V \text{ pre fault}$
 $\Delta I = I \text{ post} - I \text{ pre fault}$

The $\int \Delta V \times \Delta I$ signals which have almost zero amplitude at steady state operation of the system, initially changed to a negative value for faults seen in forward direction or to a positive for the backward direction.

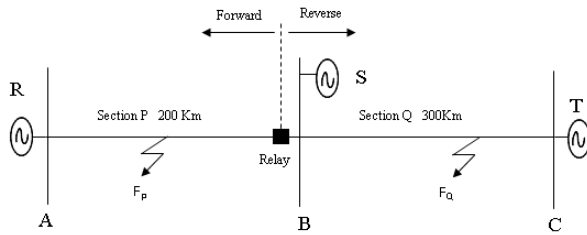


Figure 2 Model of the simulated system.

When a fault F_p single phase to ground (B-G) occur far 150Km from busbar A on section P as in figure 2 , the measurement at relay shown in figure 3 of S where the polarity of S is negative which mean that the fault seen by relay as forward fault

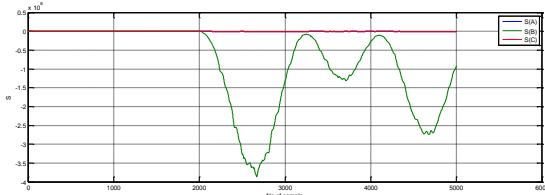


Figure 3 Shows the measurement of S at relay of a (B -G) fault

When a fault F_Q single phase to ground (B-G) occur far 250Km from busbar B on section Q as in figure 2 , the measurement at relay shown in figure 4 of S where the polarity of S is positive which mean that the fault seen by relay as backward fault

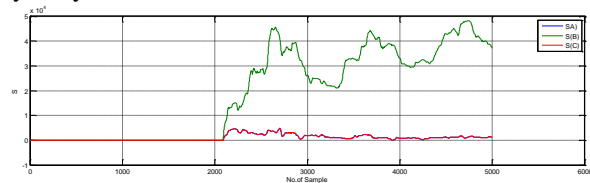


Figure 4 Shows the measurement of S at relay of a (B -G) fault

2.2. Determination of the Fault Type

To discriminate if the faulted phase is grounded or not another algorithm is added to detect the fault type and it is performed by getting the ground mode of by using Clarke transform

$$\text{Where } \Delta S_0 = \frac{1}{3}(\Delta S_a + \Delta S_b + \Delta S_c) \quad (2)$$

The presence of $\int \Delta S_0$ indicates the fault is grounded, otherwise it is ungrounded.

When a fault F_Q single phase to ground (B-G) occur far 150Km from busbar A on section P as in figure 2 , the measurement at relay shown in figure 5 of $\int \Delta S_0$ where the presence of $\int \Delta S_0$ indicates the fault is grounded

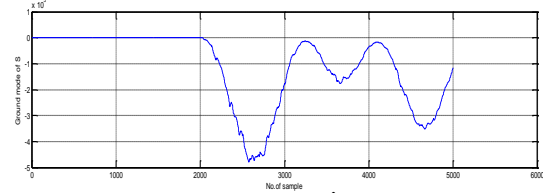


Figure 5 Shows the measurement of $\int \Delta S_0$ at relay of a (B -G) fault

When a fault F_Q double phase fault(A-B) occur far 150Km from busbar A on section P as in figure 2 , the measurement at relay shown in figure 6 of $\int \Delta S_0$ where there is no presence of $\int \Delta S_0$ indicates the fault is ungrounded

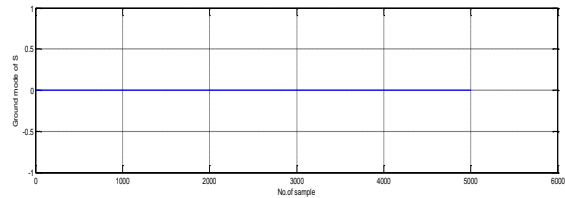


Figure 6 shows the measurement of $\int \Delta S_0$ at relay of a (A-B) fault

2.3. Discrimination of Fault Position

2.3.1. One zone distance protection

The distance relay is characterized by having two measuring circuits that measure the feeder current and the feeder voltage at the relaying point. The impedance seen by the relay is calculated as the ratio between the voltage and the current values measured by the relay measuring circuits.

The one zone distance relay will operate when the magnitude of the impedance seen by the relay is less than the line impedance.

We can use one of the impedance calculations in Table 1 to estimate the fault location.

TABLE 1
SIMPLE IMPEDANCE EQUATIONS

Fault type	impedance
A-ground	$V_a / (I_a + mI_0)$
B-ground	$V_b / (I_b + mI_0)$
C-ground	$V_c / (I_c + mI_0)$
a-b or a-b-g	V_{ab} / I_{ab}
b-c or b-c-g	V_{bc} / I_{bc}
c-a or c-a-g	V_{ca} / I_{ca}
a-b-c	Any of the following : V_{ab} / I_{ab} , V_{bc} / I_{bc} , V_{ca} / I_{ca}

The challenges for accuracy of one-ended fault location are well known and are described in several sources [21] [22] [23] [24]. To summarize, the following conditions can cause errors for one-ended impedance-based fault location methods[25]:

- Combined effect of fault resistance and load
- System infeeds
- Inaccurate relay measurement, instrument transformer or line parameters.

As the impedance of the fault is almost always resistive, it might be assumed that the fault resistance has no effect on the reactance relays. In a radial system this is generally true, but not necessarily if the fault is fed from two or more points since the voltage drop in the fault resistance is added to the drop in the line and affects the relay voltage. If the fault resistance is large in comparison to the line reactance the effect could be serious and this type of relay should not be used. [26] So the reactance and impedance algorithm cannot use in presences of fault resistance, so the one zone distance protection algorithm can use in ungrounded fault. Fault classification used to select which equation can be used from table 1 where the fault classification used for ungrounded fault as in fig.(7) which include the fault classification and impedance equation for each fault type, which uses the equation (1) for classification.

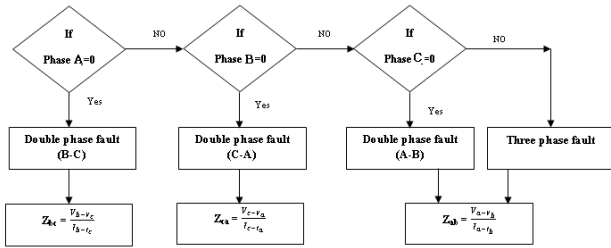


Figure 7 Flow chart of fault classification for ungrounded fault

2.3.2. Principle of TW based fault location

2.3.2.1. Discrete Wavelet Transform (DWT)

Wavelet transform is one of the best tools to depict transients generated by a fault on power systems. Unlike the Fourier transform which presents some information about frequency of a signal, the wavelet transform gives some information about both frequency and time of a given signal.

Taking this feature of WT into account, it is possible to detect the time of occurrence of fault transients.

Before preparation of a signal for decomposing into different scales with different levels of resolution using wavelet transform, a three-phase signal should be transformed into three independent modal components. It can be done by a modal transformation. Clarke's matrix as one of the transformation matrices can decouple the phase signals into modal components.

$$\begin{bmatrix} I_0 \\ I_1 \\ I_2 \end{bmatrix} = \frac{1}{3} \begin{bmatrix} 1 & 1 & 1 \\ 2 & -1 & -1 \\ 0 & \sqrt{3} & -\sqrt{3} \end{bmatrix} \begin{bmatrix} I_a \\ I_b \\ I_c \end{bmatrix}$$

The modal components consist of a ground mode (I_0), an aerial mode 1 (I_1) and an aerial mode 2 (I_2) components.

As mentioned earlier, the best tool for analyzing the transients generated by fault, which contain high-frequency and are often nonperiodic, is wavelet transform; therefore, it is an alternative to the Fourier techniques.

Wavelet transform is largely due to this technique, which can be efficiently implemented by using only two filters, one high pass (HP) and one low pass (LP) at level (k). The results are down-sampled by a factor two and the same two filters are applied to the output of the low pass filter from the previous stage[27]. The high pass filter is derived from the wavelet function (mother wavelet) and measures the details in a certain input. The low pass filter on the other hand delivers a smoothed version of the input signal and is derived from a scaling function, associated to the mother wavelet.

DWT is the discrete version of the Wavelet analysis and is defined by the equation

$$W(j, k) = \sum \sum u(k) 2^{-j/2} \phi(2^{-j} n - k) \quad (3)$$

Where $u(k)$ is the mother wavelet. DWT is a kind of multi resolution analysis, where the signal is analyzed at different frequencies with different resolutions. The analyzed signal is then decomposed into approximation and detail coefficients. The approximation coefficients are further decomposed into another set of approximation and detail coefficients. The process is then repeated and the successive stages of decomposition are known as level-1, level-2, etc. The detail coefficient of level 1 (D1) contains the high frequency information of the signal. The choice of mother wavelet plays a significant role in the analysis and B spline mother wavelet has been adopted in this paper. The WTCs are obtained using MATLAB wavelet transform toolbox.

2.3.2.2. TW base fault location

Figs.8, 9 show the Lattice diagrams of aerial and ground mode TWs for grounded faults in the middle and the end of protected transmission line, respectively.

- Let $\Delta t_{L_f/2}$ represent the interval for ground and aerial mode in the middle of the line as shown in figure 8

$$\Delta t_{L_f/2} = \frac{L_f}{2} \left[\frac{1}{v_0} - \frac{1}{v_1} \right] \quad (4)$$

Where v_0 is the velocity of the ground mode
(192 km/ms)
 v_1 is the velocity of the Ariel mode
(287.2 km/ms)
 L_f is the length of the protected line

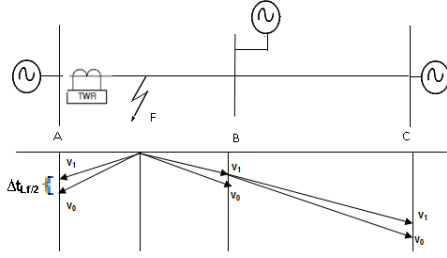


Figure 8 Grounded fault in the middle line

- Let Δt_x represent the practical interval for ground and aerial mode to propagate over the distance from the fault point to the measurement bus

$$\Delta t_x = X \left[\frac{1}{v_0} - \frac{1}{v_1} \right] \quad (5)$$

- If $\Delta t_x < \Delta t_{L_f}/2$

$$\text{So } X \left[\frac{1}{v_0} - \frac{1}{v_1} \right] < \frac{L_f}{2} \left[\frac{1}{v_0} - \frac{1}{v_1} \right]$$

$$\text{So } X < L_f/2$$

This case indicates the fault occurred in the half line near the measurement terminal

- Let Δt_{L_f} represent the interval for ground and aerial mode in the end of the line as shown in figure 9

$$\Delta t_{L_f} = L_f \left[\frac{1}{v_0} - \frac{1}{v_1} \right] \quad (6)$$

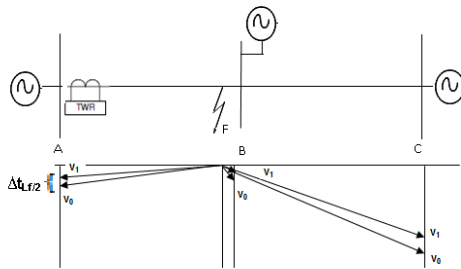


Figure 9 Grounded fault in the end of line

- If $\Delta t_{L_f} > \Delta t_x > \Delta t_{L_f}/2$

$$\text{Where } \Delta t_{L_f} = 2 \Delta t_{L_f}/2$$

$$\text{So } 2 \Delta t_{L_f}/2 > \Delta t_x > \Delta t_{L_f}/2$$

$$\text{By dividing on } \Delta t_{L_f}/2$$

$$2 > \frac{\Delta t_x}{\Delta t_{L_f}/2} > 1$$

When the ratio $\left(\frac{\Delta t_x}{\Delta t_{L_f}/2} \right)$ is greater than 1 and less

than 2 so the fault occur in the second half of the protected line , if the ratio is greater than 2 so the fault occur outside the protected line seen as external fault

3. SIMULATION STUDY AND RESULTS ANALYSIS

To evaluate the validity of the above algorithm, a typical 500kV EHV frequency-dependent transmission line model is simulated by MATLAB/ Simulink.

Transmission system is shown in Fig.10. The system consists of two sections of a transmission line with lengths of 200 and 300 km, respectively, where three busbars , and are supplied by power sources with short circuit capacity at levels of R,S and T of 52, 26, and 10 GVA respectively.

The simulation has been carried out to evaluate the proposed scheme into the measured relay installed at the end of R with consideration of a variety of fault conditions: fault position, fault path resistance, fault inception angle, fault type.

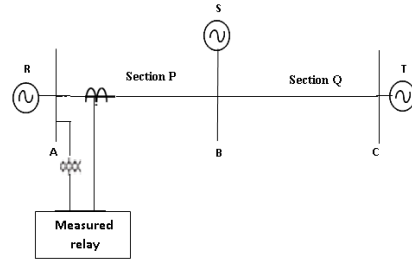


Figure 10 Model of the simulated system.

A. Response to a Single-Phase-Earth Fault

In actual circumstances, single-phase-earth fault is of representation in respect that it accounts for most of the fault cases.

Fig.11 to Fig.14 illustrate some typical single-phase-earth fault outputs using travelling wave algorithm above at $T_f=0.02$ sec, where the intervals between ground and Ariel modes and relay responses are shown.

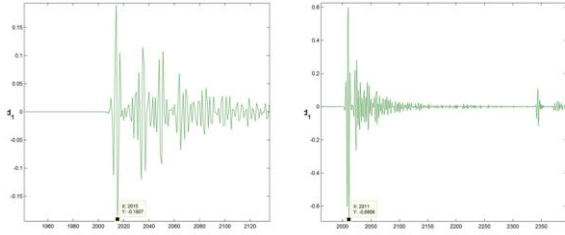


Figure 11 A phase-a-earth fault at 20km from busbar A on section P

In fig.11 The first peaks can be easily detected as 0.02015 sec for ground mode and 0.02011 sec for aerial mode .then the interval between them is 0.04 ms and since

$$\Delta t_{L_f/2} = \frac{200}{2} \left(\frac{1}{192} - \frac{1}{287.2} \right) = 0.172ms$$

Then $\Delta t_x < \Delta t_{L_f/2}$ which dedicates the fault occurred in the first half of protected line (internal fault)

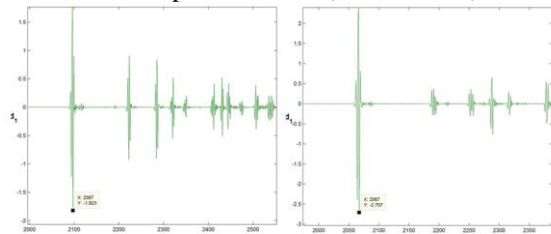


Figure 12.A phase-a-earth fault at 180km from busbar A on section P

In fig.12 The first peaks can be easily detected as 0.02097 sec for ground mode and 0.02067 sec for aerial mode .then the interval between them is 0.3 ms and since

Then $\Delta t_x < \Delta t_{L_f/2}$, But $\frac{\Delta t_x}{\Delta t_{L_f/2}} = 1.744 < 2$ which

dedicates the fault occurred in the second half of the protected line (internal fault)

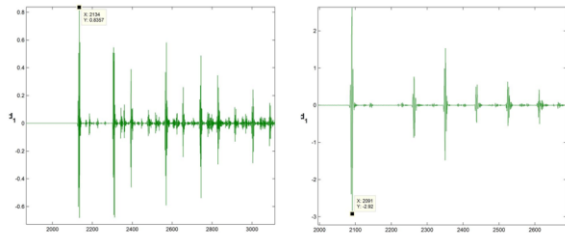


Figure 13. A phase-a-earth fault at 50km from busbar B on section Q

In fig.13 The first peaks can be easily detected as 0.02134 sec for ground mode and 0.02091 sec for aerial mode .then the interval between them is 0.43 ms and since

Then $\Delta t_x > \Delta t_{L_f/2}$, But $\frac{\Delta t_x}{\Delta t_{L_f/2}} = 2.5 > 2$ which

dedicates the fault occurred outside the protected line (external fault)

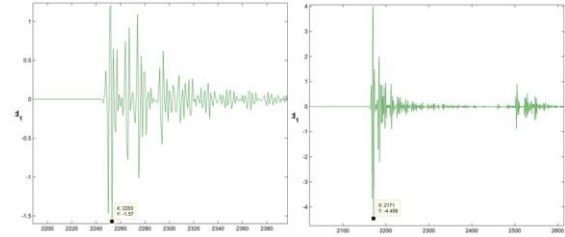


Figure 14. A phase-a-earth fault at 280km from busbar B on section Q

In fig.14 The first peaks can be easily detected as 0.02253 sec for ground mode and 0.02171 sec for aerial mode .then the interval between them is 0.82 ms and since

Then $\Delta t_x > \Delta t_{L_f/2}$, But $\frac{\Delta t_x}{\Delta t_{L_f/2}} = 4.76 > 2$ which

dedicates the fault occurred outside the protected line (external fault)

B. Response to Single-Phase-Earth Fault with Fault Path Resistance

The response of the relay to a phase-A-earth fault with fault path resistance 25 Ω at 180km from busbar A on section P is shown in Fig.15. The result indicates that with the increase of fault path resistance, the corresponding magnitudes are diminished in comparison with direct fault as Fig.12.

Nevertheless, the characteristics still remain similar. The first peaks can be easily detected as 0.02097 sec for ground mode and 0.02067 sec for aerial mode .then the interval between them is 0.3 ms

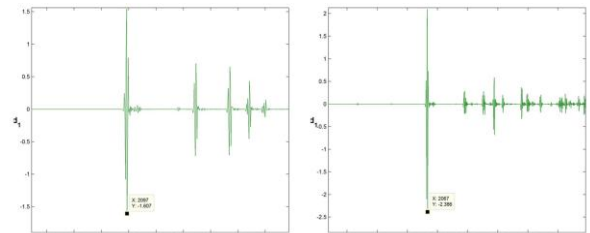


Fig.15. A phase-a-earth fault with fault resistance 25 Ω at 180km from busbar A on section P

C. Response to Single-Phase-Earth Fault with Fault inception angle 90°

The response of the relay to a phase-A-earth fault with fault inception angle 90 °at 180km from busbar A on section P is shown in Fig.16.

In fig.16 the first peaks can be easily detected as 0.02597 sec for ground mode and 0.02567 sec for aerial mode .then the interval between them is 0.3 ms and since

Then $\Delta t_x < \Delta t_{L_f} / 2$, But $\frac{\Delta t_x}{\Delta t_{L_f} / 2} = 1.744 < 2$ which

dedicates the fault occurred in the second half of the protected line (internal fault)

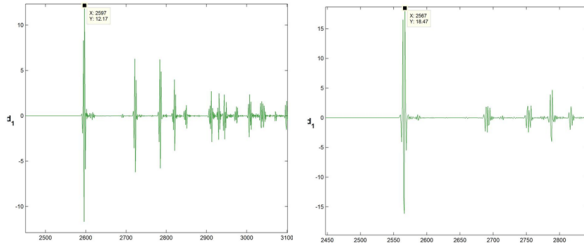


Fig.16. A phase-a-earth fault with fault inception angle 90° at 180km from busbar A on section P

D. Response to a Double-Phase Fault

Fig.17 to Fig.20 illustrate the response of the relay to a phase a-b earth fault using one zone distance protection algorithm above, where the measured impedance and relay responses are shown.

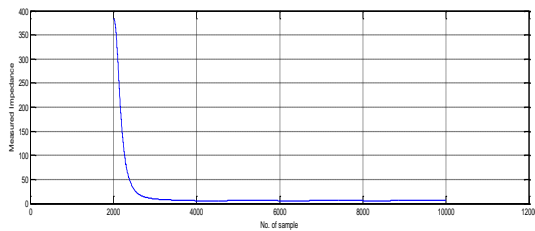


Fig.17. A double phases(a-b)fault at 20km from busbar A on section P

In fig. 17 The measured impedance after one cycle 5.8 ohm where the line impedance 60.6 ohm

Then $Z_m > Z_L$ which dedicates the fault occurred inside the protected line (internal fault)

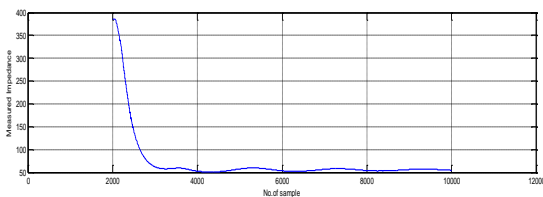


Fig.18. A double phases(a-b)fault at 180km from busbar A on section P

In fig. 18 The measured impedance after one cycle 52.4 ohm where the line impedance 60.6 ohm

Then $Z_m > Z_L$ which dedicates the fault occurred inside the protected line (internal fault)

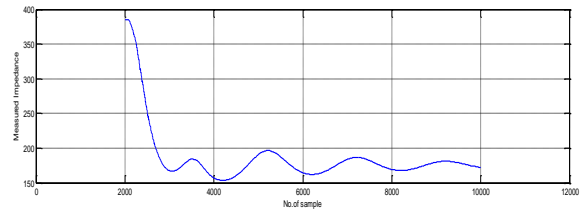


Fig.19. A double phase(a-b)fault at 50km from busbar B on section Q

In fig. 19 The measured impedance after one cycle 157.2 ohm where the line impedance 60.6 ohm

Then $Z_m > Z_L$ which dedicates the fault occurred outside the protected line (external fault)

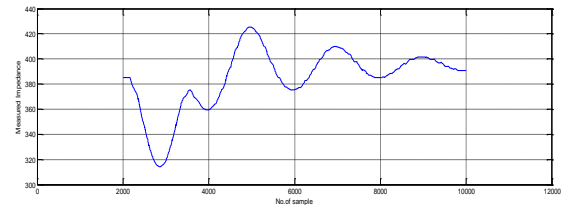


Fig.20. A double phase(a-b)fault at 280km from busbar B on section Q

In fig. 20 The measured impedance after one cycle 359.5 ohm where the line impedance 60.6 ohm

Then $Z_m > Z_L$ which dedicates the fault occurred outside the protected line (external fault)

4 CONCLUSIONS

This paper examined how the measured impedance at the relay location and the fault generated high frequency transients wavefronts can be combined in a single relay to find solutions for the negative features associated with each method when applied independently. This is improve both speed and reliability of the distance protection scheme.

The protection algorithm developed for this scheme provides the directional fault detections with ability of phase selection that discriminates between phases involved in inception of the faults.

The one zone distance protection algorithm developed for this scheme provides the possibility of complete line length protection

The travelling waves initiated by a fault depend not only on the fault position but also on the fault type, the fault inception angle, fault impedance.

The simulation carried out on a simple 500 KV three phase power system indicates that the proposed protection scheme is able to reliably detect the faults in the protection zone and remains secured for the faults outside the protection zone.

References

- [1] Protective Relay Application Guide, 3rd Edition. GEC Alsthom T&D Protection and Control, St Leonards Works, Stafford UK, 1990
- [2] Detection of high impedance fault using adaptive non-communication protection technique, Z.Q. Bo, X.Z. Dong, S.X. Shi, Z. Gan, B.R.J. Cauce Power Engineering Society Summer Meeting, 2002 IEEE;
- [3] Crossley PA, Gale PF, Bingyin Xu, Yaozhong Ge, Cory B.J, Barker JRG. (1993) Fault location based on travelling waves. Fifth International Conference on Developments in Power System Protection, Conference Publication No. 368, 54-59.
- [4] Crossley P.A. & MacLaren P.G. (1983) Distance protection based on travelling waves. IEEE Transactions on Power Apparatus and System 102 (9): 2971-2983.
- [5] Ancell G.B. & Pahalawaththa N.C. (1994). Maximum likelihood estimation of fault location on transmission lines using travelling waves. IEEE Transactions on Power Delivery 9(2): 680-689.
- [6] Jie Liang, Elangovan S., Devotta J.B.X. (1999) Adaptive travelling wave protection algorithm using two correlation functions. IEEE Transactions on Power Delivery, 14(1): 126-131.
- [7] Bo Z.Q., Weller G., Redfern M.A. (1999) Accurate fault location technique for distribution system using fault-generated high-frequency transient voltage signals. IEE Proceedings - Generation, Transmission and Distribution 146(1): 73 – 79.
- [8] Crossley P.A., Gale P.F, Aurangzeb M. (2001) Fault location using high frequency travelling waves measured at a single location on a transmission line. Developments in Power System Protection, Amsterdam, Holland, 9-12 April, 403-406.
- [9] Elhaffar, A., Lehtonen, M. (2004) Travelling waves based earth fault location in 400 kV transmission network using single end measurement. Large Engineering systems Conference on Power Engineering, LESCOPE-04, 28-30 July, 53 – 56.
- [10] Thomas, D.W.P., Christopoulos, C., Tang, Y., Gale, P., Stokoe, J. (2004) Single ended travelling wave fault location scheme based on wavelet analysis. Eighth IEE International Conference on Developments in Power System Protection, Volume 1, 5-8 April, 196 – 199.
- [11] Zeng Xiangjun, Li, K.K., Liu Zhengyi, Yin Xianggen (2004) Fault location using traveling wave for power networks. Industry Applications Conference, 2004, 39th IAS Annual Meeting, 3-7 October, 2426 – 2429.
- [12] Evrenosoglu, C.Y., Abur, A. (2005) Travelling wave based fault location for teed circuits. IEEE Transactions on Power Delivery 20(2):1115 – 1121.
- [13] Gale P.F. and Giannattasio B.F. (1994) Travelling waves get to the point. Modern Power Systems :45-47.
- [14] P. Gale and R. Burnett, “A study of power line response to lightning using GPS based travelling wave fault locators and the US national lightning detection network,” presented at the Proc. Fault and Disturbance Analysis and Precise Measurements Power Systems Conf., Arlington, VA, 1996.
- [15] A. Abur and F. Magnago, “Fault location using wavelets,” IEEE Trans. Power Del., vol. 13, no. 4, pp. 1475–1480, Oct. 1988.
- [16] D. Spoor and J. G. Zhu, Improved Single-Ended Traveling-Wave Fault-Location Algorithm Based on Experience with Conventional Substation Transducers, IEEE Transactio
- [17] Bashir, M. Niazy, I. Sadeh, J. Taghizadeh, M. Considering Characteristics of Arc on Travelling Wave Fault Location Algorithm for the Transmission Lines Without Using Line Parameters
- [18] IEEE Std C37.114: ‘IEEE Guide for Determining Fault Location on AC Transmission and Distribution Lines’, 2004
- [19] Choi, M.S., Lee, S.J., Lim, S.I., Lee, D.S. and Yang, X.: ‘A Direct Three-Phase Circuit Analysis-Based Fault Location for Line-to-Line Fault’, IEEE Trans. on Power Deliv., Oct. 2007, 22, (4), pp. 2541-7
- [20] Novel Approach for Single Ended Fault Location in Allusion to Unbalanced Transmission Lines, Proceedings of the 7th IET International Conference on Advances in Power System Control, Operation and Management (APSCOM 2006), Hongkong
- [21] IEEE Standard PC37.114, “Draft Guide For Determining Fault Location on AC Transmission and Distribution Lines,” 2004.
- [22] T. Takagi, Y. Yamakoshi, M. Yamaura, R. Kondou, and T. Matsushima, “Development of a New Type Fault Locator Using the One-Terminal Voltage and Current Data,” IEEE Transactions on Power Apparatus and Systems, Vol. PAS-101, No. 8, August 1982, pp. 2892-2898.
- [23] Edmund O. Schweitzer, III, “A Review of Impedance-Based Fault Locating Experience,” Proceedings of the 15th Annual Western Protective Relay Conference, Spokane, WA, October 24-27, 1988.
- [24] D.A. Tziouvaras, J.B. Roberts, G. Benmouyal, “New Multi-Ended Fault Location Design For Two- or Three-Terminal Lines,” presented at CIGRE Conference, 1999, <http://www.selinc.com/techpprs/6089.pdf>.
- [25] Karl Zimmerman and David Costello, Schweitzer “Impedance-Based Fault Location Experience” 58th Annual Conference for Protective Relay Engineers, pp. 211–226, 2005.

- [26] Protection of Electricity Distribution Networks (2nd Edition) Gers, Juan M.; Holmes, Edward J. © 2004 Institution of Engineering and Technology
- [27] Ngu. E-E and Ramar, K, "A Combined Impedance and Traveling Wave Based Fault Location Method for Multi-terminal Transmission Lines", International Journal of Electrical Power and Energy Systems (IJEPES), November, 2011, pp.1767-1775